Fizika Nizkikh Temperatur, 2010, v. 36, No. 5, p. 504–511

Local formation of HArF in solid argon: Low-temperature limit and thermal activation

H. Lignell*, L. Khriachtchev, A. Lignell**, and M. Räsänen

Laboratory of Physical Chemistry, P.O. Box 55, FIN-00014 University of Helsinki, Finland
E-mail: leonid.khriachtchev@helsinki.fi

Received January 12, 2010

The H + Ar + F reaction leading to HArF formation in an argon matrix is studied at temperatures down to 8 K. The effects of the precursor concentration, deuteration, IR light, and deposition temperature as well as thermal activation of this reaction are studied. It is found that HArF molecules are formed slowly but efficiently at 8 K in a photolyzed HF/Ar matrix, supporting the previously reported results. The formation rate of HArF (and DArF) exhibits a low-temperature limit and enhances at elevated temperatures with activation energy of ca. 40 meV. All the data show that HArF is formed as a result of a local reaction of hydrogen atoms with the parent Ar–F centers and the tunneling mechanism is very probable here. The locality of the precursor photolysis required for this tunneling reaction is consistent with the partial HArF formation observed during photolysis of HF in an argon matrix. The decay mechanism of $(ArHAr)^+$ cations is also studied. The present results confirm the previous conclusions that the decay of the cations is not essentially connected to the HArF formation.

PACS: **33.15.–e** Properties of molecules;
82.33.Pt Solid state chemistry;
82.50.Hp Processes caused by visible and UV light.

Keywords: noble-gas chemistry, matrix isolation, quantum tunnelling.

1. Introduction

Noble-gas hydrides with the general formula HNgY (H = hydrogen atom, Ng = noble-gas atom, and Y = = electronegative fragment) have been studied both experimentally and computationally [1–5]. These molecules have an $(HNg)^+Y^-$ charge-transfer character leading to a strong absorption of the H–Ng stretching mode. They can be prepared using photolysis of a hydrogen-containing precursor HY in a noble-gas matrix followed by thermal annealing promoting the H + Ng + Y reaction of the neutral fragments [6,7]. Some of these molecules (HArF, HXeNCO, and HKrCl) are observed in relatively small amounts during UV photolysis as an intermediate species indicating locality of solid-state photodissociation [8–10].

HArF is a ground-state neutral molecule of argon [9,11]. It is synthesized experimentally using photolysis and annealing of HF in solid argon. HArF is an example of a noble-gas hydride forming during photolysis, hence indicating the locality of HF photolysis in solid argon. After thermal annealing, HArF can occupy two different matrix configurations referred as unstable HArF and stable HArF [11,12]. The unstable HArF configuration is formed in the largest amounts at ca. 20 K. Annealing above ca. 28 K decomposes unstable HArF leaving only the stable configuration visible.

The HArF molecule has been widely studied by using theoretical methods. For example, the structure, potential energy surface, and vibrational properties have been examined [13–17]. A number of studies have simulated the trapping configurations of HArF in an argon matrix [18–20]. Recently Bochenkova *et al*. have reported theoretical and experimental results on libration motion of HArF in solid argon (Ref. 21) and on thermal reorganization of the unstable to stable HArF configuration [22].

It has been found experimentally that HArF molecules are formed slowly after photolysis of HF/Ar matrices at temperatures down to 8 K (without annealing) [23]. It has been suggested that this «low-temperature» formation of HArF molecule occurs at a short-range scale and the reaction mechanism probably involves quantum tunneling of hydrogen. Local (short-range) processes have been often discussed in connection with noble-gas hydrides. Pettersson *et al*. have shown that the formation of HXeI molecule originates from a combination of local and global H atom mobilities [24]. Moreover, the recovery of HXeCC and

* Current address: Department of Chemistry, University of California, Irvine, CA 92697-2025, USA
** Current address: Jet Propulsion Laboratory, California Institute of Technology, 4800 Oak Grove Drive, Pasadena, CA 91109, USA

HXeI after IR decomposition are local processes presumably involving quantum tunneling of hydrogen atoms [6,7]. The local mechanism of the HArF formation seems to be different from the cases of other HNgY molecules in Kr and Xe matrices formed mainly upon global mobility of hydrogen atoms activated by thermal annealing [25]. To investigate the question of the HArF formation scale is the main motivation of the present work. We study here the HArF formation at temperatures down to 8 K evaluating the formation kinetics, HF/Ar concentration dependence, effects of IR light and deposition temperature, H/D isotope effect, and activation energy of the formation. This information sheds light on the HArF formation mechanism.

Another subject related to the current work is the decay of the $(NgHNg)^+$ cations in noble-gas matrices. This phenomenon has been known for many years and various mechanisms have been suggested [23,25–27]. It has been shown that the HArF formation and the decay of $(ArHAr)^+$ are kinetically different suggesting that these two phenomena are fundamentally unconnected [23]. However, the decay of $(ArHAr)^+$ and $(ArDAr)^+$ occur at 8 K with similar rates to the formation of HArF and DArF, respectively, and more studies in this direction are clearly needed. Here, we report new experimental results on the ion decay supporting the previous conclusions.

2. Experimental details

The HF/Ar solid matrices were studied in a closed-cycle helium cryostat (APD, DE 202A) providing temperatures down to 8 K. The matrices were deposited onto a cold CsI substrate by passing argon gas (99.9999% AGA) through HF-containing pyridine polymer (Fluka) using the method developed previously [9]. The deposition temperature varied between 8 and 16 K, most of the matrices being deposited at 12 K. A sulphuric acid H_2SO_4 drop (J.T. Baker 95–97%) was added into the deposition line to remove impurity water from the sample-gas flow. Deuteration of HF was made by using a drop of deuterated sulphuric acid D_2SO_4 (Merck 96–98%, D-degree > 99%) in the deposition line and the achieved degree of deuteration was up to 90% [9]. After deposition, the matrices were photolyzed at 8 K with a krypton lamp (Opthos, microwave power 40 W) emitting 127–160-nm light. The ratio between HF and the matrix gas (Ar) was varied by changing the amount of pyridine polymer and the argon flow rate through the deposition line. The absolute concentrations of HF and DF in the matrices are difficult to control with this preparation method. However, the HF/Ar matrix ratio can be estimated using the integrated molar absorptivity of gaseous HF (99.8 km/mol) [28,29], and the HF/Ar ratios were typically ~1:2000. In some experiments, the HF and DF amounts were comparable and the HArF, $(ArHAr)^+$, DArF, and $(ArDAr)^+$ species were studied simultaneously. The decomposition of HF after 30–60 min irradiation with a Kr lamp was typically ~20% and practically no progress was achieved for longer exposures. The HF decomposition is probably limited due to photolysis-induced absorbers and scattering in the optically thick matrix [30]. The IR absorption spectra in the 4000 to 400 cm^{-1} range with resolution of 1 cm^{-1} were measured with a Nicolet SX60 FTIR spectrometer.

3. Experimental results

The IR spectra of HF and DF in an Ar matrix are presented in Fig. 1. The monomeric HF bands are located at 3962.2 and 3953.6 cm^{-1}, the weak Q branch is at 3920.6 cm^{-1}, and the $(HF)_2$ absorption is at 3826.3 cm^{-1}. DF absorbs at 2895.1 cm^{-1} and $(DF)_2$ at 2803.5 cm^{-1}. These bands are in agreement with the literature data [31]. Photolysis with a Kr lamp decreases these bands and builds up the $(ArHAr)^+$ absorptions [32]. Some amount of HArF is seen already after photolysis as pointed out earlier [9,12].

Figure 2,*a* shows the HArF formation upon annealing the photolyzed matrices. Unstable HArF has triplet absorption of the H–Ar stretching mode at 1965.7, 1969.4, and 1972.3 cm^{-1} and the absorptions of stable HArF are at 2016.3 and 2020.8 cm^{-1} [11,12]. The unstable and stable HArF configurations are related to different local matrix morphologies [20]. Annealing at 20 K produces the maxi-

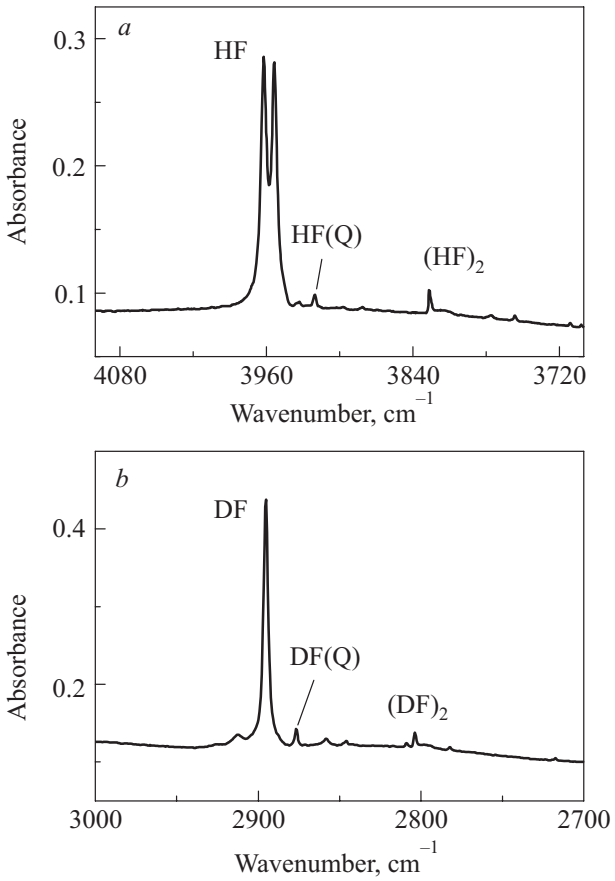

Fig. 1. IR spectra of HF (*a*) and DF (*b*) in an Ar matrix. The spectra are measured at 8 K.

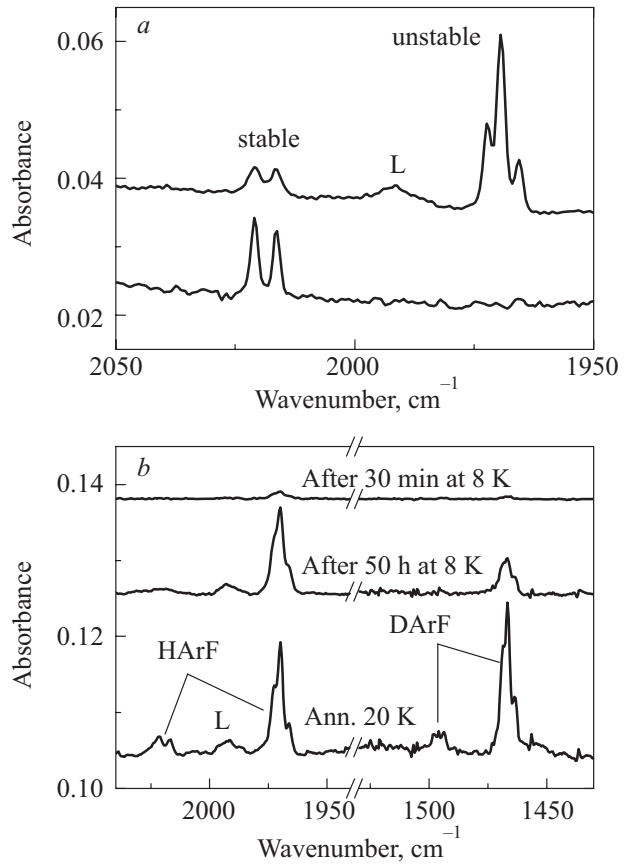

Fig. 2. (*a*) Formation of HArF upon thermal annealing. In the upper trace (annealing at 20 K), both unstable and stable configurations are present. In the lower trace (annealing at 30 K), only the stable form is present [11,22]. (*b*) Low-temperature formation of HArF and DArF [23]. The upper trace is measured after 30 min at 8 K and the middle trace after 50 h at 8 K after photolysis. Notice that the unstable configuration of HArF is mainly formed at 8 K. The lower trace shows the situation after additional annealing of the matrix at 20 K. The band marked with *L* is due to the librational motion of the HArF molecule in solid argon [21]. The spectra are measured at 8 K. The HF(DF)/Ar matrix was preliminarily photolyzed with a Kr lamp. The photolysis-induced HArF absorptions are subtracted from the spectra shown in panel (*b*).

mum amount of unstable HArF. The thermally unstable configuration converts to the more stable configuration upon annealing at higher temperatures due to the relaxation of the matrix surrounding [11,12,22]. The broad feature marked with *L* has been recently assigned to librational motion of HArF in solid argon by Bochenkova *et al*. [21]. A similar phenomenon was previously found for HXeBr and HKrCl in Xe and Kr matrices, respectively [33].

As reported previously, HArF forms slowly even at the lowest experimental temperature of 8 K [23]. In the present work, we study this process in more detail, evaluating its dependence on various experimental parameters. Figure 2,*b* shows the formation of HArF and DArF at 8 K (two upper spectra). No recovery of HF is observed after long period at low temperatures. Annealing of the matrix at 20 K after long period at 8 K does not increase the HArF concentration much, i.e., the formation process can be mostly completed even at 8 K. In other words, the long low-temperature formation leads to nearly the same amount of unstable HArF as short annealing at 20 K (see Fig. 2,*b*). It should be noticed that the low-temperature (~10 K) process produces HArF mainly in the unstable configuration. The thermally-activated transition of unstable to stable HArF was studied elsewhere [22].

The formation of unstable DArF at 8 K is very slow compared to HArF (by a factor of ~50 at 8 K, see Fig. 3,*a*), which agrees with the previous measurements [23]. Due to this isotope effect, it is difficult to finish the DArF formation process at 8 K in real experiments. The HArF and DArF formation rates increase at elevated temperatures

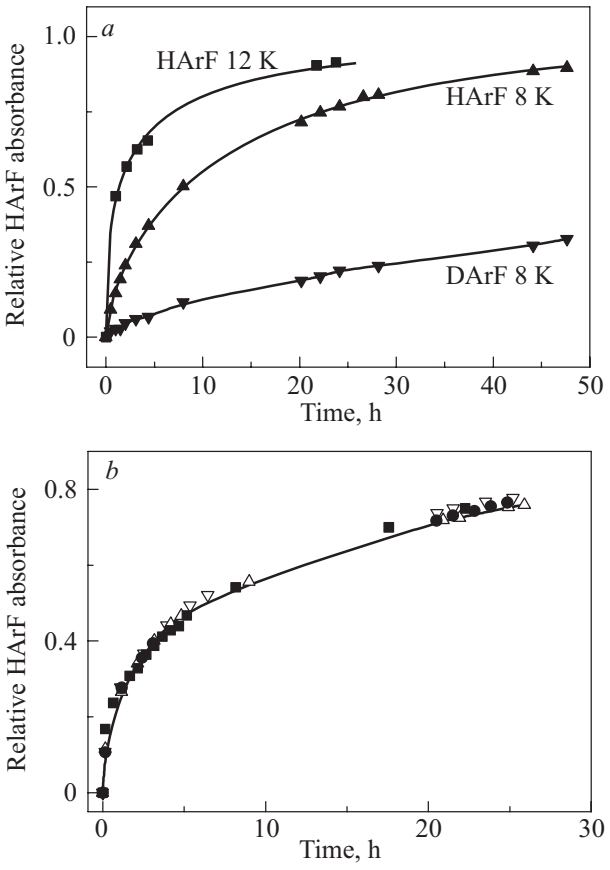

Fig. 3. (*a*) Formation of unstable HArF as a function of time at different temperatures (8 and 12 K). Formation of unstable DArF is shown at 8 K (down triangles) demonstrating a strong isotope effect. The spectra were measured at the annealing temperatures. The lines are stretched-exponential fits. (*b*) Demonstration of the negligible effect of IR light on the HArF formation at 10 K. The solid and open symbols present the data obtained with the closed and open Globar source between the measurements, respectively. The integrated absorbance was normalized by the value obtained after annealing at 20 K and the values after photolysis were subtracted. These experiments were done using relatively low HF concentrations (~1:2500).

(see Fig. 3,*a*). The possible effect of broadband IR light was studied by measuring the HArF formation under the Globar light and in the dark. The formation rates in these two cases were found to be very similar as shown in Fig. 3,*b* for formation of HArF at 10 K.

The matrix deposition temperature affects the HArF formation rate at low temperatures. The HArF formation kinetics was studied at 10 K for matrices deposited at 8, 12, and 16 K. The HArF formation was fastest for deposition at 8 K and slowest for deposition at 16 K. The difference between the formation rates was substantial (several times). In order to eliminate this factor of uncertainty, we mainly analyzed the data obtained for deposition at 12 K.

The $(ArHAr)^+$ ions are generated by photolysis and slowly decay after the formation (see Fig. 4), and this process shows a strong isotope effect. While the $(ArHAr)^+$ ions practically disappear after 8 h at 8 K, the $(ArDAr)^+$ decay is minor after 50 h at 8 K remaining small even after annealing the sample for several minutes at 20 K. The decay of the ions enhances at elevated temperatures but less efficiently than the simultaneous HArF formation (see Fig. 5).

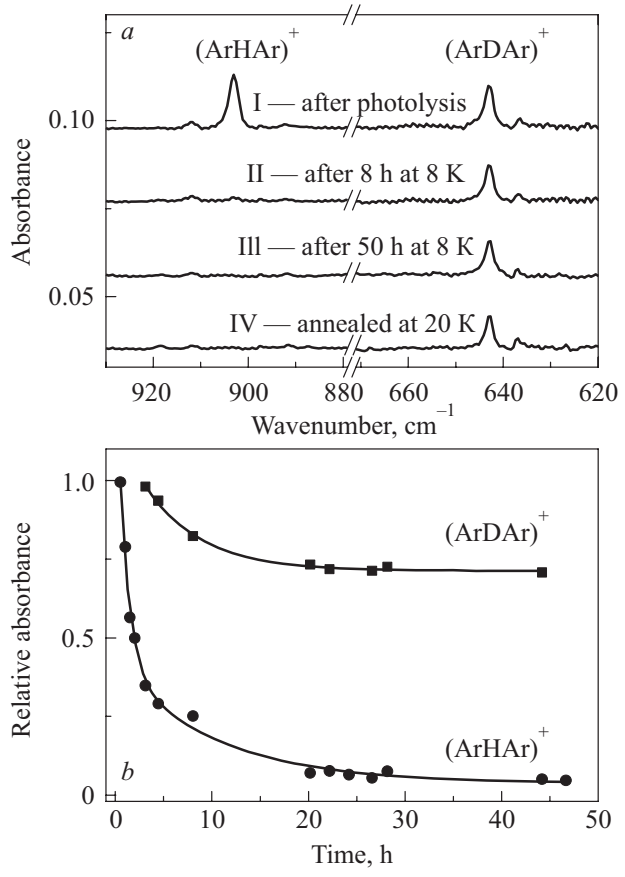

Fig. 4. (*a*) IR spectra of $(ArHAr)^+$ and $(ArDAr)^+$. Spectrum I is obtained after irradiation. Spectra II and III represent the situations 8 and 50 h after photolysis. Spectrum IV is recorded after annealing the sample at 20 K. The spectra were measured at 8 K. (*b*) Decay of $(ArHAr)^+$ and $(ArDAr)^+$ in an Ar matrix at 8 K. The data were normalized by the values obtained after photolysis.

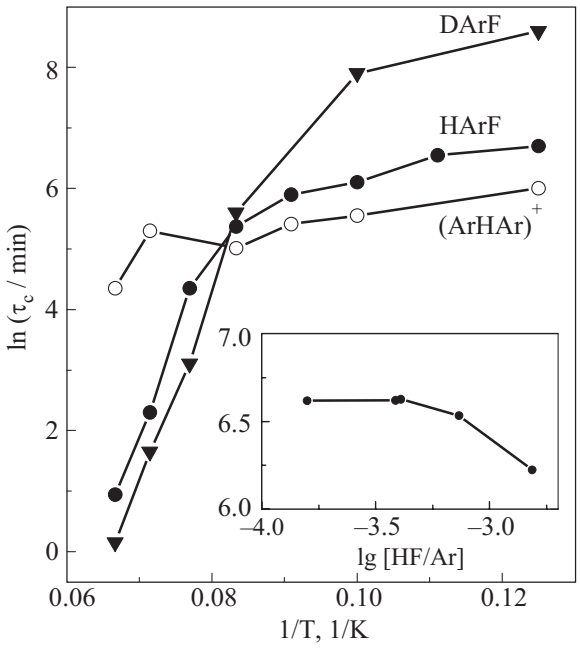

Fig. 5. Arrhenius plot for the formation of unstable HArF and DArF and decay of $(ArHAr)^+$. The unstable HArF and DArF formation time was estimated at 0.63 and 0.45 levels of the integrated intensity obtained after annealing at 20 K, respectively. The insert shows the HF-precursor concentration dependence of the HArF formation at 10 K. The Ar/HF ratios were estimated using the molar absorptivity of gaseous HF [29].

Practically no effect of Globar irradiation on the $(ArHAr)^+$ decay is observed. The decay time of the ions is measured at the 1/*e* level of concentration observed after photolysis.

Figure 5 presents the Arrhenius plot for the HArF and DArF formation (unstable configuration) in matrices deposited at 12 K with the HF/Ar ~1/2000 ratio. The formation time at various temperatures is calculated at the 0.63 level of the HArF concentration after additional annealing at 20 K similarly to the previous studies of other HNgY molecules [34,35]. It is a characteristic time for a single exponential process and can be used for more complicated kinetics functions as well [36]. The DArF formation time is presented at the 0.45 level of the maximal value obtained by annealing at 20 K because, due to the very slow formation, the 0.63 level is not achieved in these experiments. The Arrhenius plots for the HArF and DArF formation are quite different. The formation of DArF is much slower compared to HArF at 8 K whereas the formation rates are comparable at 15 K. The activation energy of the DArF formation was estimated by using four high-temperature data points of the Arrhenius plots yielding (322 ± 18) cm^{-1}, and the three data points for HArF lead to the same value of (333 ± 25) cm^{-1}.

The concentration dependence of the HArF formation was studied by varying the amount of the precursor HF (see insert in Fig. 5). We found that the lower HF precursor concentrations (1:1400 to 1:6000) did not affect the forma-

tion kinetics. For highly concentrated samples (~1:700) the formation is somewhat faster.

4. Discussion

The HArF formation can be in principle a global or local process with respect to atomic mobility, and thermal mobilization of both H and F atoms is possible. Local (short-range) formation efficiency is controlled by the local formation barrier that can be intrinsic (characteristic of a molecule in vacuum) or matrix-induced. The intrinsic barrier can be caused by the avoided crossing between the ionic and neutral potential energy surfaces, which enables the HArF formation from the H + Ar + F neutral fragments. The calculated intrinsic formation barrier is 0.18 eV by Runeberg *et al.* [14] and 0.44 eV by Li *et al*. [16]. Bihary *et al.* have obtained that the H + Ar + F reaction barrier decreases by ca. 0.2 eV in solid argon with respect to the process in vacuum and estimated a barrier of ~0.3 eV for the H + Ar + F reaction in solid argon [15]. It should be admitted that reaction barriers in matrices are very complicated to model due to many particles involved into the process. Intuitively, the precursor photodissociation and the HArF formation can be affected by specific local matrix morphology. The local processes in solid state are energetically different from the global (long-range) processes [22,37]. Global (long-range) formation occurs via atomic diffusion over relatively long distances (compared to the lattice parameter), and the formation reaction most probably occurs apart from the parent cage. Formation of HKrCl in a Kr matrix and formation of HXeCCH and HXeBr in a Xe matrix have been shown to be mainly global processes [25,35], although some contribution from local mobility can also be noticed [24].

The concentration dependence of the formation rate is a good probe for the local (*vs*. global) formation process. For a local process, no dependence on the precursor concentration should take place. In contrast, the global formation should become slower for lower concentrations of the reacting species because more jumps are needed to meet the reactive center. The experimental dependence of the HArF formation time on the HF precursor concentration is shown in the insert in Fig. 5. It is observed that the lower (from 1:6000 to 1:1400) HF precursor concentrations have practically no effect on the HArF formation time, which suggests the local formation mechanism. For example, the HKrCl formation time changed between these precursor concentrations by a factor of two, which was attributed to the global formation mechanism [35]. For higher HF/Ar concentrations (~1:700), the formation time decreases by ca. 30%. To explain the concentration dependence, one can speculate that matrices with higher HF concentrations have more defects, and this may lower the formation barrier compared to a defect-free matrix. This change is also much smaller than in the case of the HKrCl formation at similar precursor concentrations. It should be remembered that the concentration dependence of the formation time can also be weakened by high losses of mobile atoms [25], which complicates the comparison of different experiments.

The local formation of HArF is reasonable because of the locality of HF photolysis in solid argon, which is evidenced by HArF absorptions observed after UV photolysis. In this model, a part of dissociating H atoms stays very near the parent cage and they can be captured in the HArF energy minimum hence forming the intermediate. These HArF intermediate molecules can be destroyed by next photons, providing large excess energy to H atoms and driving them further away from the parent cages. Another part of dissociating H atoms can in principle be stabilized in the matrix promptly after the first dissociation event. The ratio between these two channels of the secondary (via HArF intermediate) and direct stabilization of H atoms in the matrix is difficult to measure and it presumably depends on the excess energy and matrix material (see Ref. 10 for more discussion). It is possible that the H atoms, stabilized in the matrix via decomposition of HArF intermediates, do not participate in the low-temperature formation of HArF due to a longer-scale separation from the parent cages. If the dissociation via intermediates is a major channel, a large part of H atoms could be lost for the HArF formation at low temperatures. On the other hand, these H atoms may form HArF at elevated temperatures via longer-range mobility; however, this formation channel is evidently not dominating.

It should be understood that our claim on local formation of HArF does not reject the long-range mobility of hydrogen atoms in solid argon. It is possible that H atoms can globally move in a perfect argon crystal; however, no indication for this mobility has been presented, to our knowledge, in literature and it is not evidenced by the present results either. In accord, Vaskonen *et al*. observed an efficient geminate recombination of HBr after UV photolysis in solid argon, which also featured the locality of solid-state photolysis and short-range recovery of HBr [38]. In the present case, the recovery of HF does not occur because this channel is suppressed by the HArF formation.

The dependence of the formation time on the deposition temperature (slower formation for higher deposition temperature) is consistent with the concept of the local formation mechanism. In this model, higher deposition temperatures lead to more regular matrix structures providing deeper energy wells for atoms stabilized after photolysis and consequently higher reaction barriers. In the previous work, the increase of deposition temperature led to a higher temperature of the unstable to stable HArF transformation [11], which probably originated from local mobility of vacancies [12,22]. No formation of stable HArF is observed at the lowest experimental temperatures; hence, thermal mobilization of vacancies is required for the un-

stable to stable HArF transition with the experimental activation energy of ca. 70 meV [22].

The Arrhenius plot for the HArF and DArF formation is shown in Fig. 5. The dependence consists of two parts: a plateau for lower temperatures and a thermally activated part above 12 K. The temperature dependence with a low-temperature limit is characteristic for a quantum tunneling mechanism [39,40]. The classical contribution to chemical reactions is negligible at low temperatures and quantum tunneling dominates. It was found out by Goldanskii *et al.* that chemical reactions involving light particles do not stop even at zero temperature, which is called a low-temperature limit of a chemical reaction rate [39]. The other support for the tunneling mechanism is the large H/D isotope effect, showing a much slower process for deuterium (see Fig. 3,*a*) [40]. The H/D isotope effect also shows that the HArF formation (unstable configuration) is not essentially contributed by mobility of F atoms and matrix vacancies.

Bihary *et al.* have calculated that the potential barrier for the formation of HArF in solid argon from the neutral H + Ar + F fragments is ~0.3 eV with the width of 1.3 Å [15]. In our opinion, this barrier is consistent with the observed HArF formation rates taking into account the hydrogen tunneling rates for the *cis* to *trans* process in carboxylic acids having similar reaction barriers [40]. Furthermore, it has been suggested previously that HXeI and HXeCC recover via tunneling of hydrogen after IR decomposition [6,7]. We suppose that the tunneling mechanism is very probable for the HArF formation, which contradicts with the theoretical conclusions of Bihary *et al*. [15]. Importantly for the present study, tunneling of hydrogen atoms may occur only through a short distance, which further evidences the locality of both the HF photodissociation and HArF formation in solid argon. It looks plausible that HArF is formed at low temperatures from the same H atoms as upon annealing at 20 K. This conclusion is supported by the stability of the HArF concentration upon annealing at 20 K after a long period at 8 K. On the other hand, some amount of unstable HArF is probably reorganized to stable HArF at this temperature [22], but hopefully it is not the dominating channel.

The thermal activation of the DArF formation is observed at somewhat lower temperatures than that of HArF and at 14–15 K HArF and DArF are formed with similar rates. The Arrhenius plots give the activation energy of ~300 cm^{-1} (40 meV) for the HArF and DArF formation. The mechanism of this thermal activation is not easy to interpret. This energy is much higher than that of a single-phonon process in solid argon (ca. 10 meV). At the first glance, it is inconsistent with the reaction over energy barrier calculated by Bihary *et al.* (0.3 eV) [15]. However, this computational barrier may be inaccurate so that we cannot completely exclude an over-barrier reaction. Moreover, efficient tunneling can occur below the barrier (by ca. 0.1 eV), hence the effective barrier can be lower than the calculated one [41]. For the H + XeC_2 reaction, the experimental activation energy was remarkably similar to the present case [7]. Next, the tunneling reaction can be activated by population of some higher energy state; however, the nature of such a state is unclear. Resonance with the accepting state of HArF may also play a role. Finally, the tunneling process might be enhanced by reorganization of the matrix medium. The relaxed surrounding geometries are different before and after tunneling reaction, and this mismatch can slow down the tunneling process, which is much faster than the reorganization of heavy atoms. Temperature may help the surrounding to find geometry better suitable for tunneling, which increases the tunneling rate. For instance, this reorganization may involve local mobility of vacancies. Bochenkova *et al.* have recently calculated barriers for vacancy mobility around HArF molecule in an argon cluster, and the smallest activation energy (45 meV) [22] was close to the activation energy obtained here. However, the formation of unstable HArF has not been modeled and more theoretical effort is required to understand this activation mechanism.

Another interesting question is the relationship between the formation of HArF and the decomposition of $(ArHAr)^+$. The neutralization of $(ArHAr)^+$ upon electron transfer from F^- might in principle ignite the formation of HArF via the H + Ar + F reaction [23]. However, these two processes have different kinetics showing that they are not directly connected. In the present work we fitted the HArF formation and $(ArHAr)^+$ decay data at 8 K with a stretched-exponential function and found different parameters for these two processes, in agreement with the previous conclusions of Ref. 23 on their independency. Even a stronger support of our model is provided by the Arrhenius plot shown in Fig. 5. It is clearly seen that the HArF formation and $(ArHAr)^+$ decay possess very different temperature dependences: the $(ArHAr)^+$ decay is much less sensitive to the matrix temperature. Furthermore, the decay of $(ArDAr)^+$ is much slower (by orders of magnitude) than the DArF formation at 20 K (see Fig. 4). Because of this very slow process, we could not obtain experimental data for the Arrhenius plot of the $(ArDAr)^+$ decay.

5. Concluding remarks

We have studied experimentally the low-temperature formation of HArF in various experimental conditions, including the concentration dependence, deuteration, and effect of IR light. The thermal activation of the process was also measured. The decay of $(ArHAr)^+$ cations was studied and its hypothetical connection with the HArF formation was discussed and finally rejected.

It has been found that HArF molecules in the unstable configuration are formed in major amounts after a long period at 8 K in a photolyzed HF/Ar matrix, which is in basic agreement with the earlier report [23]. The Arrhenius

plot shows a strong H/D isotope effect (about two orders of magnitude) and a low-temperature limit of the HArF formation. The activation energy for the HArF and DArF formation is ca. 40 meV, and it is presumably connected with the mobility of hydrogen atoms (not F atoms or vacancies). Several mechanisms are possible for this enhancement including activation of vacancy mobility in the matrix surrounding. All the data show that HArF forms in a local reaction of H atoms with the parent Ar–F centers and tunneling mechanism is very probable as supported by the observed strong deuteration effect and the low-temperature limit of the reaction. The locality of the precursor photolysis required for this tunneling phenomenon is consistent with the HArF formation during photolysis of HF in solid argon [12].

The decay mechanism of $(ArHAr)^+$ cations in an Ar matrix has been recently discussed in terms of tunneling of an electron from an electronegative fragment to the $(ArHAr)^+$ cations [23,25]. This process was tentatively demonstrated for synchronous neutralization of $(KrHKr)^+$ and $CCCN^-$ in a Kr matrix [42]. In this model, the electron tunnels over a relatively long distance to the cation, and this process does not lead to recombination of the neutralized fragments to a noble-gas hydride. The present work supports the previous conclusions since the kinetic data for the formation of HArF and decay of $(ArHAr)^+$ and thermal activation of these processes are different, especially for the deuterated species.

Acknowledgments

The Academy of Finland supported this work partially through the Finnish Center of Excellence in Computational Molecular Science. H. L. is a member of the graduate school Laskemo (Ministry of Education, Finland). We thank Mika Pettersson for helpful discussions and Toni Nurminen for technical assistance.

1. L. Khriachtchev, M. Räsänen, and R.B. Gerber, *Acc. Chem. Res*. **42**, 183 (2009).
2. A. Lignell and L. Khriachtchev, *J. Mol. Struct*. **889**, 1 (2008).
3. A. Lignell, L. Khriachtchev, J. Lundell, H. Tanskanen, and M. Räsänen, *J. Chem. Phys*. **125**, 184514 (2006).
4. S.A.C. McDowell, *Curr. Org. Chem*. **10**, 791 (2006).
5. J. Lundell, L. Khriachtchev, M. Pettersson, and M. Räsänen, *Fiz. Nizk. Temp*. **26**, 923 (2000) [*Low Temp. Phys*. **26**, 680 (2000)].
6. M. Pettersson, J. Nieminen, L. Khriachtchev, and M. Räsänen, *J. Chem. Phys*. **107**, 8423 (1997).
7. L. Khriachtchev, H. Tanskanen, and M. Räsänen, *J. Chem. Phys*. **124**, 181101 (2006).
8. M. Pettersson, L. Khriachtchev, J. Lundell, S. Jolkkonen, and M. Räsänen, *J. Phys. Chem*. **A104**, 3579 (2000).
9. L. Khriachtchev, M. Pettersson, N. Runeberg, J. Lundell, and M. Räsänen, *Nature (London)* **406**, 874 (2000).
10. L. Khriachtchev, M. Pettersson, J. Lundell, and M. Räsänen, *J. Chem. Phys*. **114**, 7727 (2001).
11. L. Khriachtchev, M. Pettersson, A. Lignell, and M. Räsänen, *J. Am. Chem. Soc.* **123**, 8610 (2001).
12. L. Khriachtchev, A. Lignell, and M. Räsänen, *J. Chem. Phys.* **120**, 3353 (2004).
13. J. Lundell, G.M. Chaban, and R.B. Gerber, *Chem. Phys. Lett*. **331**, 308 (2000).
14. N. Runeberg, M. Pettersson, L. Khriachtchev, J. Lundell, and M. Räsänen, *J. Chem. Phys*. **114**, 836 (2001).
15. Z. Bihary, G.M. Chaban, and R.B. Gerber, *J. Chem. Phys.* **119**, 11278 (2003).
16. H. Li, D. Xie, and H. Guo, *J. Chem. Phys*. **120**, 4273 (2004).
17. A. Avramopolous, H. Reis, J. Li, and M. G. Papadopolos, *J. Am. Chem. Soc*. **126**, 6179 (2004).
18. Z. Bihary, G.M. Chaban, and R.B. Gerber, *J. Chem. Phys.* **116**, 5521 (2002).
19. S. Jolkkonen, M. Pettersson, and J. Lundell, *J. Chem. Phys.* **119**, 7356 (2003).
20. A.V. Bochenkova, D.A. Firsov, and A.V. Nemukhin, *Chem. Phys. Lett.* **405**, 165 (2005).
21. A.V. Bochenkova, L. Khriachtchev, A. Lignell, M. Räsänen, H. Lignell, A.A. Granovsky, and A.V. Nemukhin, *Phys. Rev*. **B77**, 094301 (2008).
22. A.V. Bochenkova, V.E. Bochenkov, and L. Khriachtchev, *J. Phys. Chem.* **A113**, 7654 (2009).
23. L. Khriachtchev, A. Lignell, and M. Räsänen, *J. Chem. Phys*. **123**, 064507 (2005).
24. M. Pettersson, L. Khriachtchev, R.-J. Roozeman, and M. Räsänen, *Chem. Phys. Lett*. **323**, 506 (2000).
25. H. Tanskanen, L. Khriachtchev, A. Lignell, M. Räsänen, S. Johansson, I. Khyzhniy, and E. Savchenko, *Phys. Chem. Chem. Phys.* **10**, 692 (2008).
26. M. Beyer, E.V. Savchenko, and V.E. Bondybey, *Fiz. Nizk. Temp*. **29**, 1045 (2003) [*Low Temp. Phys*. **29**, 792 (2003)].
27. A. Lignell, L. Khriachtchev, H. Lignell, and M. Räsänen, *Phys. Chem. Chem. Phys*. **8**, 2457 (2006).
28. A.S. Pine, A. Fried, and J.W. Elkins, *J. Mol. Spectrosc*. **109**, 30 (1985).
29. M. Pettersson, L. Khriachtchev, A. Lignell, M. Räsänen, Z. Bihary, and R.B. Gerber, *J. Chem. Phys*. **116**, 2508 (2002).
30. L. Khriachtchev, M. Pettersson, and M. Räsänen, *Chem. Phys. Lett*. **288**, 727 (1998).
31. M.G. Mason, W.G. Von Holle, and D.V. Robinson, *J. Chem. Phys*. **54**, 3491 (1971).
32. V.E. Bondybey and G.C. Pimentel, *J. Chem. Phys*. **56**, 3832 (1972).
33. L. Khriachtchev, A. Lignell, J. Juselius, M. Räsänen, and E. Savchenko, *J. Chem. Phys*. **122**, 014510 (2005).
34. L. Khriachtchev, H. Tanskanen, M. Pettersson, M. Räsänen, V. Feldman, F. Sukhov, A. Orlov, and A.F. Shestakov, *J. Chem. Phys*. **116**, 5708 (2002).
35. L. Khriachtchev, M. Saarelainen, M. Pettersson, and M. Räsänen, *J. Chem. Phys*. **118**, 6403 (2003).
36. J. Eberlein and M. Creuzburg, *J. Chem. Phys*. **106**, 2188 (1997).

37. L. Khriachtchev, M. Pettersson, S. Pehkonen, E. Isoniemi, and M. Räsänen, *J. Chem. Phys*. **111**, 1650 (1999).
38. K. Vaskonen, J. Eloranta, T. Kiljunen, and H. Kunttu, *J. Chem. Phys*. **110**, 2122 (1999).
39. V.I. Goldanskii, M.D. Frank-Kamenetskii, and I.M. Barkalov, *Science* **182**, 1344 (1973).
40. L. Khriachtchev, *J. Mol. Struct*. **880**, 14 (2008).
41. M. Pettersson, E.M.S. Macoas, L. Khriachtchev, R. Fausto, and M. Räsänen, *J. Am. Chem. Soc*. **125**, 4058 (2003).
42. L. Khriachtchev, A. Lignell, H. Tanskanen, J. Lundell, H. Kiljunen, and M. Räsänen, *J. Phys. Chem*. **A110**, 11876 (2006).